Title
Biocompatible Chemotherapy for Leukemia by Acid-Cleavable, PEGylated FTY720.

Journal
Bioconjugate chemistry, 31(3)

ISSN
1043-1802

Authors
Kemp, Jessica A
Keebaugh, Andrew
Edson, Julius A
et al.

Publication Date
2020-03-01

DOI
10.1021/acs.bioconjchem.9b00822

Bioconjugate Chemistry

pubs.acs.org/bc Article

Biocompatible Chemotherapy for Leukemia by Acid-Cleavable, PEGylated FTY720

Jessica A. Kemp, Andrew Keebaugh, Julius A. Edson, David Chow, Michael T. Kleinman, Yap Ching Chew, Alison N. McCracken, Aimee L. Edinger, and Young Jik Kwon*

Cite This: *Bioconjugate Chem.* 2020, 31, 673–684 Read Online

ACCESS | Metrics & More | Article Recommendations | Supporting Information

ABSTRACT: Targeting the inability of cancerous cells to adapt to metabolic stress is a promising alternative to conventional cancer chemotherapy. FTY720 (Gilenya), an FDA-approved drug for the treatment of multiple sclerosis, has recently been shown to inhibit cancer progression through the down-regulation of essential nutrient transport proteins, selectively starving cancer cells to death. However, the clinical use of FTY720 for cancer therapy is prohibited because of its capability of inducing immunosuppression (lymphopenia) and bradycardia when phosphorylated upon administration. A prodrug to specifically prevent phosphorylation during circulation, hence avoiding bradycardia and lymphopenia, was synthesized by capping its hydroxyl groups with polyethylene glycol (PEG) via an acid-cleavable ketal linkage. Improved aqueous solubility was also accomplished by PEGylation. The prodrug reduces to fully potent FTY720 upon cellular uptake and induces metabolic stress in cancer cells. Enhanced release of FTY720 at a mildly acidic endosomal pH and the ability to substantially down-regulate cell-surface nutrient transporter proteins in leukemia cells only by an acid-cleaved drug were confirmed. Importantly, the prodrug demonstrated nearly identical efficacy to FTY720 in an animal model of BCR-Abl-driven leukemia without inducing bradycardia or lymphopenia in vivo, highlighting its potential clinical value. The prodrug formulation of FTY720 demonstrates the utility of precisely engineering a drug to avoid undesirable effects by tackling specific molecular mechanisms as well as a financially favorable alternative to new drug development. A multitude of existing cancer therapeutics may be explored for prodrug formulation to avoid specific side effects and preserve or enhance therapeutic efficacy.

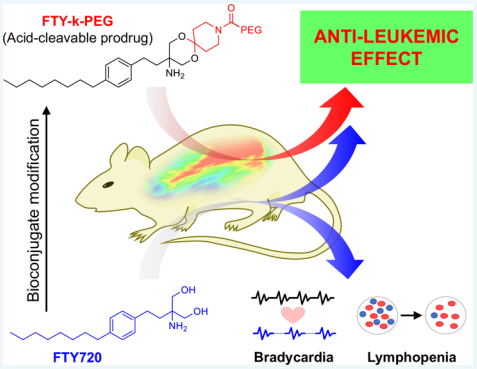

INTRODUCTION

While modern medicine has made great advances in the fight against highly challenging diseases such as cancer, a need for specificity remains. Chemotherapeutics target cellular processes which are ubiquitously required, albeit to different extents, in all cells, thereby killing a subset of healthy cells and causing adverse side effects.[1] Furthermore, these side effects severely impact patient quality of life, at times resulting in discontinuation of therapy.[2] Enhancing specificity through conjugation of targeting molecules, exploiting the tumor microenvironment, and immunotherapy show much promise in addressing systemic toxicity. However, each strategy may depend upon the particular cancer type and the patient's genetic profile, further increasing complexity in development and administration.[3−5]

A majority of targeted therapies are designed to interfere with a specific component of an oncogenic pathway; however, targets are not always specific to cancer,[6] and resistance mechanisms may activate parallel signaling pathways to allow for survival.[7,8] Cancer metabolism is an attractive therapeutic target since oncogene-driven anabolism, dysregulation of growth, and defects in autophagy sensitize cancer cells to nutrient deprivation.[9−14] Cancer cells continue biosynthesis despite nutrient deprivation, which eventually limits ATP production and induces bioenergetic stress, ultimately resulting in cell death.[15] Recent studies have reported that FTY720 (Gilenya), an FDA-approved drug for multiple sclerosis, effectively inhibits cancer progression via down-regulation of key nutrient transporters (GLUT1, ASCT2, LAT-1, and 4F2hc) and activation of protein phosphatase 2A (PP2A).[16−20] Importantly, FTY720 has shown minimal toxicity against normal cells while effectively killing cancer cells.[20,21] Under the nutrient-limiting conditions induced by FTY720, normal cells can adapt by undergoing cell cycle arrest to become quiescent and catabolic, thus maintaining survival. Although various therapies currently exist that limit access to nutrients such as angiogenesis inhibitors and L-asparaginase, many do not possess the broad applicability of FTY720.[22,23]

Received: December 4, 2019
Revised: January 14, 2020
Published: January 27, 2020

https://dx.doi.org/10.1021/acs.bioconjchem.9b00822
Bioconjugate Chem. 2020, 31, 673–684

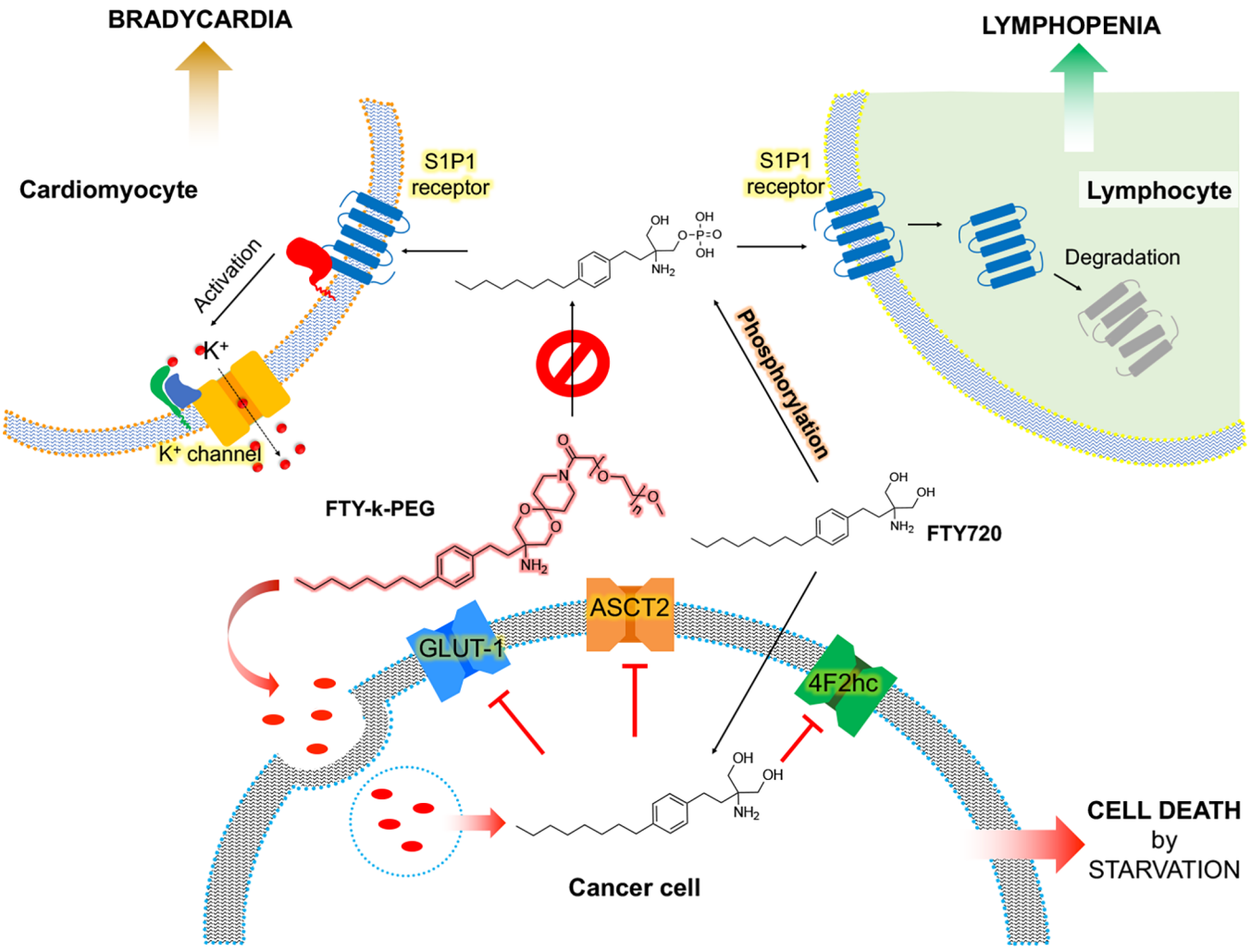

Figure 1. Hypothetical illustration of FTY-k-PEG mechanism of action. FTY720 is rapidly phosphorylated to activate S1PRs and subsequently induces bradycardia and lymphopenia at the antineoplastic dose. An acid-transforming prodrug formulation shields FTY720 from phosphorylation, while maintaining its efficacy to downregulate nutrient transport proteins once endocytosed and reduced to the antineoplastic form.

Despite its high specificity and efficacy, clinical use of FTY720 for cancer therapy is restricted due to its capability of inducing profound bradycardia at an antineoplastic dose.[24−28] FTY720 is rapidly phosphorylated and becomes an agonist for G protein-coupled sphingosine 1 phosphate receptors (S1PRs), activating a signaling cascade in atrial myocytes that reduces heart rate.[15,27−29] Furthermore, phosphorylated FTY720 is also known to induce immunosuppression by inhibiting lymphocyte egress from the thymus and secondary lymphoid organs, resulting in lymphopenia, a reduction of peripheral lymphocytes.[30] FTY720 analogues designed to prevent phosphorylation through conformational restraint were shown to eliminate these adverse effects.[20,29,31] The analogues down-regulate nutrient transport proteins and demonstrate potent anticancer efficacy in leukemia and prostate cancer models while maintaining normal heart rate. The promise of these compounds as anticancer therapies is counterbalanced by high monetary and temporal investments for new drug development. FDA approval, including clinical trials, may take up more than a decade with costs averaging over $1 billion and approval rate nearing only 10%.[32] Most importantly, this approach is not generalizable to other chemotherapeutic agents. Prodrug formulation presents a less costly alternative through the 505(b)(2) development process, which could take as few as 30 months for FDA-approval.[33,34] Therefore, a generalized approach to the development of prodrug to specifically eliminate side effects of an already approved drug is highly meritorious from a scientific and translational standpoint.

Phosphorylation of FTY720 occurs during circulation,[35−37] and a prodrug form that would be stable in the bloodstream was developed by conjugating it with a biocompatible polymer, polyethylene glycol (PEG), via an acid-labile linkage. The prodrug should avoid bradycardia and immunosuppression by limiting phosphorylation (Figure 1). Once taken up by a cancer cell via endocytosis, the prodrug transforms to its active drug in the mildly acidic endosome and induces cell death by starvation. Both in vitro and in vivo studies demonstrated that the novel molecular approach in this study addresses a key clinical demand in developing effective and safe cancer chemotherapeutics.

RESULTS AND DISCUSSION

Design and Synthesis of FTY-k-PEG. Acetals (ketals) are commonly used hydroxyl-protecting groups and ideal for prodrug formulation because of their structural versatility, facile synthesis, and tunable cleavability under mildly acid conditions.[38] The endosomal pH of ∼5.0 is an excellent

https://dx.doi.org/10.1021/acs.bioconjchem.9b00822
Bioconjugate Chem. 2020, 31, 673−684

Scheme 1. Synthesis of kFTY and FTY-k-PEG

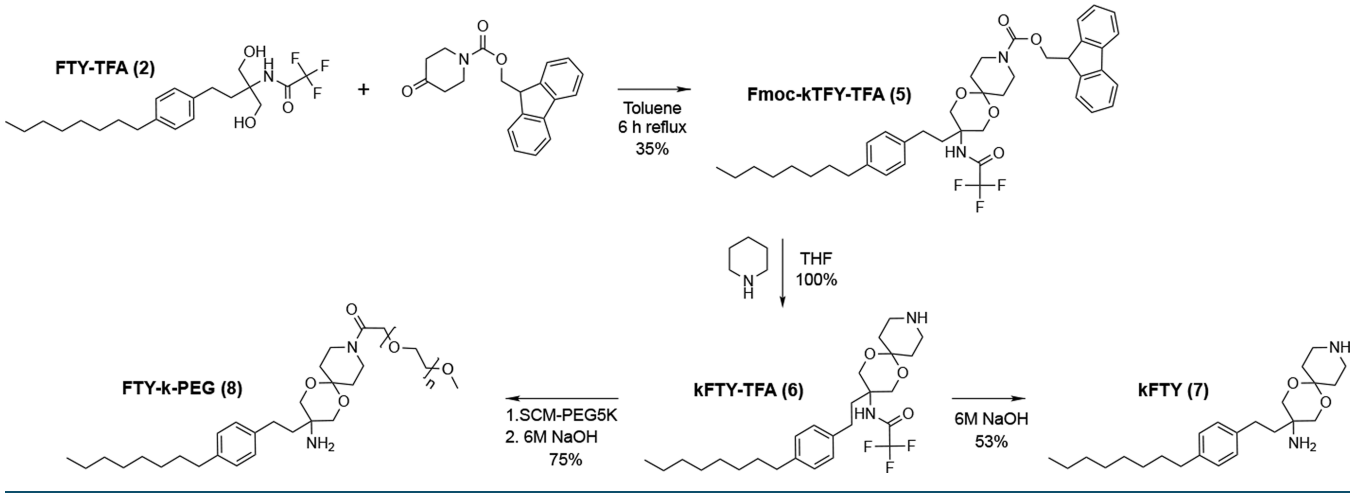

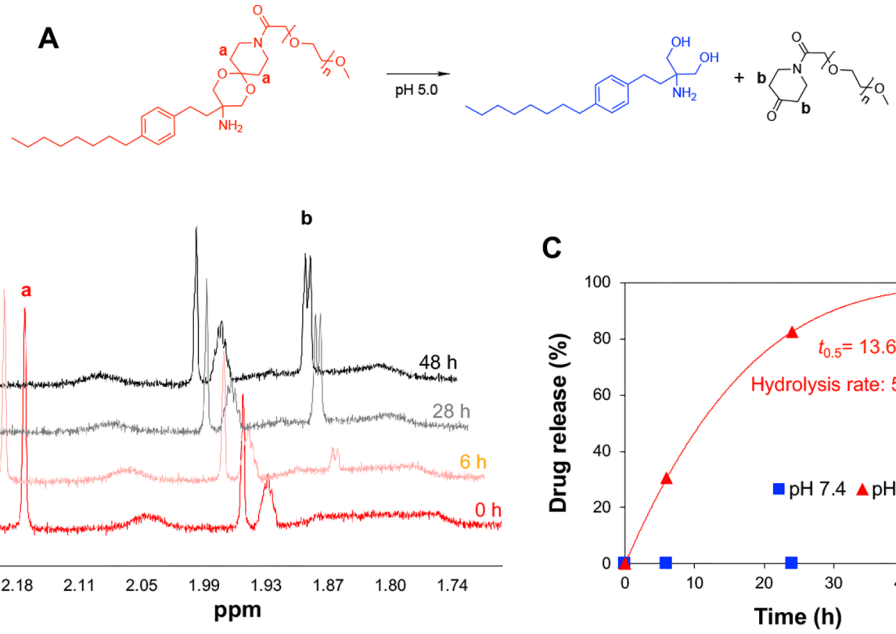

Figure 2. FTY-k-PEG efficiently hydrolyzes at a mildly acidic pH. (A) Chemical structures of FTY-k-PEG hydrolysis. (B) ^{1}H NMR spectra of FTY-k-PEG 10 mM deuterated acetate buffer pH 5.0 at 0, 6, 28, and 48 h time points. (C) Hydrolysis rate was determined by the peak shift from 2.23 to 1.91 ppm that correlates to the protons on the α-carbon of piperidone.

intracellular trigger for drug release from acid-labile drug conjugates.[39] Initial synthetic methodology utilized 2-methoxypropene to generate methyl ketal-functionalized FTY720 (mkFTY) (Scheme S1), but the addition of hydrophobic methyl groups and loss of −OH hydrogen bonding resulted in loss of water solubility. To retain the ketal moiety while increasing solubility of the prodrug, *N*-Fmoc piperidone was used to generate a cyclic ketal in kFTY (**7**) (Scheme 1), eliminating the hydrophobic methyl groups and incorporating a secondary amine as a functional handle for further conjugation. The ketal formation was achieved using azeotropic distillation by which constant removal of water efficiently drives the reaction to completion.[40,41] Although kFTY had increased water solubility compared to mkFTY, it was not readily soluble over concentrations of 10 mM. To further increase water solubility, kFTY was conjugated to succinimidyl carboxyl methyl ester polyethylene glycol (SCM-PEG 5k) prior to trifluoroacetamide (TFA)-deprotection to produce FTY-k-PEG (**8**). FTY-k-PEG was analyzed by MALDI-TOF to confirm PEGylation and TFA-deprotection (Figure S1). Average molecular weight of SCM-PEG 5K shifted by 479 Da after conjugation with kFTY-TFA (**6**) (MW 484.59 g/mol), and analysis of FTY-k-PEG (**8**) demonstrated a decrease in average molecular weight correlating to the loss of TFA (MW 97.02 g/mol). The synthetic methodology used in this synthesis proved to be straightforward and high-yielding, and it uses low-cost, commercially available materials to further increase translational value. Other macromolecules may be used for conjugation, and a plethora of stimuli-responsive linkers may be explored to further enhance the specificity and safety of an FTY prodrug. The acid-cleavable ketal linkage can be replaced by other moieties responsive to intrinsic environmental stimuli (redox, pH, etc.), external stimuli (heat, ultrasound, photoirradiation, electrochemical, magnetic, etc.), or specific biological processes (enzymatic cleavage, ion chelation, etc.), depending the molecular

https://dx.doi.org/10.1021/acs.bioconjchem.9b00822
Bioconjugate Chem. 2020, 31, 673−684

structure of a drug and the stimuli to be utilized for target indication.[39,42−48] In addition, a variety of macromolecules can also be used in lieu of PEG, including polysaccharides (i.e., hyaluronic acids), peptides, and various synthetic polymers for improved water-solubility, extended circulation, avoided premature activation, nanoparticle formulation, theranostic applications, combating resistance, and specific targeting.[49−56] The versatility of the secondary amine on kFTY would allow development of novel combination therapy by conjugating another agent (e.g., drug and contrast agent) to further enhance its anticancer properties and combined imaging and therapy.

Triggered Release of FTY720 from FTY-k-PEG under Mildly Acidic Conditions. To assess the rate of drug release and demonstrate selective release under mildly acidic conditions, FTY-k-PEG was incubated at 37 °C in 10 mM deuterated acetate and tris buffers at pH 5.0 and 7.4, respectively, over the course of 2 days. The samples were analyzed by ^{1}H NMR taken at 0, 6, 28, and 48 h (Figure 2), and rate was determined by the peak at 2.23 ppm shifting to 1.91 ppm, correlating to the α-carbon protons as piperidone re-emerged. The spectra of FTY-k-PEG indicated that FTY720 was readily released at pH 5.0 (>80% after 28 h at a rate of 51 mM/h), while no detectable hydrolysis was observed at a physiological pH of 7.4 for a few days. This suggests that FTY-k-PEG would be shielded from rapid phosphorylation during circulation and remain inactive toward S1PRs on off-target cells such as cardiomyocytes and lymphocytes, thus incapable of inducing onset bradycardia and lymphopenia. The drug release ratio at pH 5.0 to 7.4 was significantly higher than those using similar ketal chemistry.[57] This might be attributed to the hydrophobic molecular environment of cyclic ketal at a neutral pH that dramatically changes to hydrophilic upon the protonation of the proximate amine at an acidic pH, greatly facilitating acid hydrolysis.[58,59] The very slow hydrolysis of FTY-k-PEG at a neutral pH also implies reasonably long-term stability in saline, particularly under low-temperature storage conditions, in contrast to free FTY720 which requires daily fresh preparation.

Further studies in solid tumor cancer models are warranted since the tumor extracellular environment exhibits mildly acidic conditions with pH found to be as low as 5.7, a distinguishing phenotype often exploited for enhanced targeting.[60,61] Considering the dramatically triggered release of FTY720 from FTY-k-PEG at pH 5.0, in contrast to no measurable release at pH 7.4, the drug release in the tumor environment is speculated to be elevated compared with other tissues/organs.

Eradication of Cancer Cells by FTY-k-PEG via Down-Regulated Nutrient Transporter Proteins. FTY720 is known to effectively inhibit cancer progression via down-regulation of key nutrient transporters, selectively starving cancer cells to death.[20,21] mkFTY and FTY-k-PEG were analyzed for affecting the viability and down-regulation of nutrient transporter associated protein 4F2hc in BCR-Abl p190-expressing FL5.12 murine hemopoietic cells, known to have a high expression of nutrient transporters.[62] mkFTY demonstrated nearly identical efficacy to FTY720 in nutrient transporter down-regulation, confirming no loss of function after blocking hydroxyl groups by methyl ketal groups (Figure S2). FTY-k-PEG decreased expression of the amino acid transporter associated protein 4f2hc albeit at a reduced efficacy than that of FTY720 and had reduced efficacy for 24 h cell viability compared with FTY720 (Figure 3), possibly attributed to relatively inefficient cellular uptake of the PEGylated

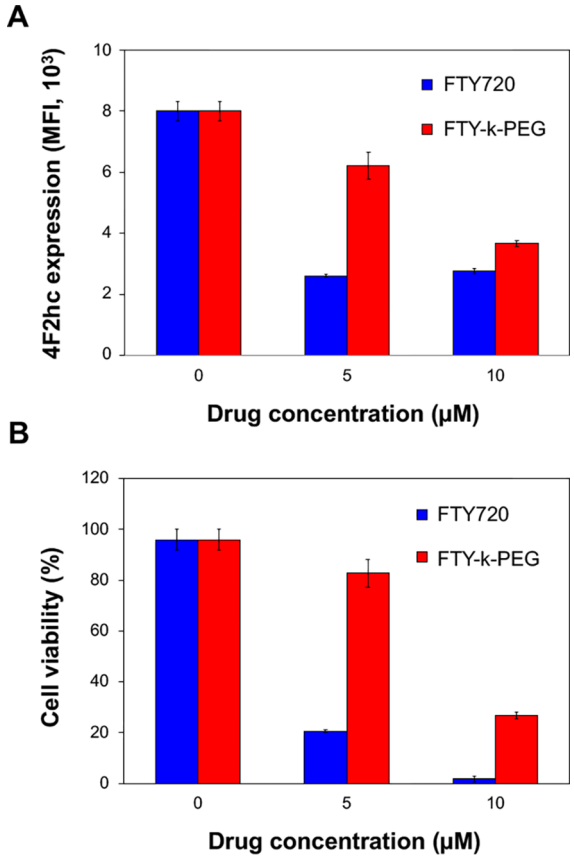

Figure 3. FTY-k-PEG down-regulates nutrient transporter 4f2hc. (A) FL5.12 cells were treated with either FTY720, FTY-k-PEG or PBS for 3 h, and surface 4f2hc expression was analyzed by flow cytometry. (B) Cell viability was assayed after 24 h treatment with PBS, FTY720, and FTY-k-PEG in BCR-Abl p190-expressing FL5.12 cells (n = 3).

prodrug[63] than the free drug and slower acid-hydrolysis of cyclic ketal than methyl ketal.[57] To confirm active drug was released selectively upon acid-hydrolysis, drugs were incubated in buffers of pH 7.4 and pH 5.0 prior to incubation with the cells (Figure 4). FTY720 was preincubated in the same buffers to rule out the possibility that the buffers would affect the drug's activity or contribute to cell apoptosis. A nonacid-cleavable, PEGylated prodrug of FTY720, FTY-PEG, was also synthesized by conjugating SCM-PEG 5k to the free amine of FTY720 via amide bond (Figure S3), known to be extremely stable and hydrolyze only under harsh conditions or enzymatic cleavage.[64]

As expected, FTY-PEG had no effect on cell viability, indicating no release of FTY720. FTY-k-PEG preincubated at pH 7.4 yielded a significant decrease in efficacy compared with FTY720, while near identical efficacy to FTY720 is observed for FTY-k-PEG preincubated at pH 5.0. This demonstrates the acid-transforming nature of FTY-k-PEG and confirms its capability of releasing active drug under mildly acidic conditions. The cells were cultured in standard media where glucose concentration is not a limiting factor. The hypoglycemic microenvironment of tumors may further enhance the metabolic stress induced by released FTY720.[65,66] The apoptotic effect of FTY720 is affected by

https://dx.doi.org/10.1021/acs.bioconjchem.9b00822
Bioconjugate Chem. 2020, 31, 673−684

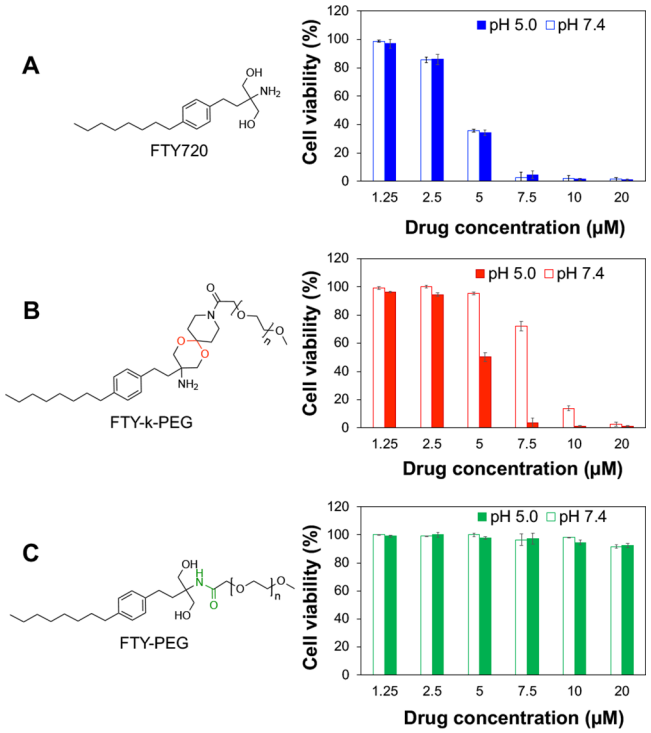

Figure 4. FTY-k-PEG demonstrates selective acid-sensitivity and in vitro efficacy. FTY720 (A), FTY-k-PEG (B), and FTYPEG (C) were incubated overnight in buffers of pH 5.0 (solid) and pH 7.4 (outline), and BCR-Abl p190-expressing FL5.12 cells were subsequently treated and assessed for viability after 24 h (n = 3).

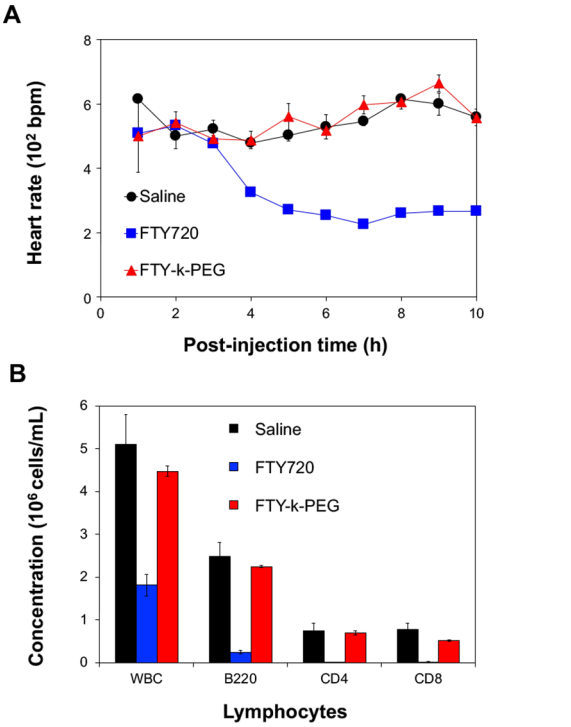

Figure 5. FTY-k-PEG avoids bradycardia and lymphopenia. (A) Heart rate was monitored for 10 h in freely moving, conscious C57/BL6 mice after i.p. administration of FTY720, FTY-k-PEG, or saline. (B) C57/BL6 mice were injected with FTY720, FTY-k-PEG, or saline, and blood was collected 12 h postinjection and analyzed for lymphocytes (n = 3).

nutrient transporter levels of cancer cells, and further studies would provide new insights in developing drugs for metabolic-dependent targeted therapy for each cancer type.

Avoided Bradycardia and Lymphopenia in Vivo by FTY-k-PEG. To test whether FTY-k-PEG avoids bradycardia, C57BL/6 mice were surgically implanted with an electrocardiographic telemetry device, and heart rate was calculated from ECG data taken in the freely moving, conscious mice after intraperitoneal (i.p.) injection of saline, FTY720, or acid-cleavable FTY-k-PEG (Figure 5A). Unmodified FTY720 clearly induces bradycardia, reducing heart rate by 50%, while FTY-k-PEG maintains normal heart rate, demonstrating that FTY-k-PEG fails to trigger bradycardia. To assess the effect of FTY-k-PEG on induction of lymphopenia, the numbers of circulating B and T lymphocytes were evaluated 12 h after i.p. injection of FTY720, FTY-k-PEG, and saline in C57BL/6 mice (Figure 5B). FTY720-induced lymphopenia was evident with nearly 60% reduction of lymphocytes, compared with that in saline or FTY-k-PEG-injected mice. These results suggest the safe administration of FTY-k-PEG at an antineoplastic dose of 155 mg/kg (10 mg/kg equivalent FTY720) without inducing the adverse effects associated with free FTY720.

Limited dosing of a chemotherapeutic agent due to adverse side effects is a significant barrier to accomplishing efficient therapy for cancer, often resulting in relapse.[67,68] The failure of FTY-k-PEG to trigger bradycardia and lymphopenia in vivo indicates a possibility of high-dose chemotherapy. In addition, because the current work focuses on elimination of side effects, further studies can include extensive evaluation of FTY-k-PEG pharmacokinetic properties and interactions of S1PRs with FTY720 vs FTY-k-PEG to elucidate biochemical understanding at a molecular level. To the best of our knowledge, this work presents a novel approach to prodrug-engineering by selectively preventing specific adverse effects through chemical modification, in contrast to many prodrugs aiming to avoid systemic side effects using a global approach. This concept could be applied to a multitude of cancer therapeutics to help decrease toxicity by evaluating detrimental side effects on a molecular level and designing prodrug moieties to prevent these unwanted effects.

Preserved Antileukemic Effect of FTY-k-PEG in Vivo. To assess the antileukemic effects of FTY-k-PEG in vivo while eliminating bradycardia and immunosuppressive activity, a BCR-Abl-driven leukemogenesis model in which FTY720 is effective was used.[21] Luciferase (Luc)-expressing, BCR-Abl p190-expressing FL5.12 (FL5.12/p190-Luc) cells were intravenously injected into Balb/c mice (1×10^5 cells/mouse), and the mice were treated daily with i.p. injections of FTY720, FTY-k-PEG, FTY-PEG (32 μmol/kg), or PBS over the course of 5 days after leukemia was established (Figure 6A). The leukemic expansion of FL5.12/p190-Luc cells was assessed by i.p. administration of synthetic firefly luciferin (120 mg/kg) and subsequent bioluminescence imaging (Figure 6B–D). There was a marked bioluminescence increase in mice treated with PBS and FTY-PEG indicating fast proliferation of BCR-Abl p190+ cells (Figure 6B,C). However, average bioluminescence signals in mice treated with FTY720 and FTY-k-PEG were 64% lower than that of PBS on day 6 ($p < 0.01$). No significant difference was observed between FTY720 and FTY-k-PEG, confirming that FTY-k-PEG maintained the antileukemic properties of FTY720 without inducing bradycardia or lymphopenia (Figure 5). These results imply that the

https://dx.doi.org/10.1021/acs.bioconjchem.9b00822
Bioconjugate Chem. 2020, 31, 673–684

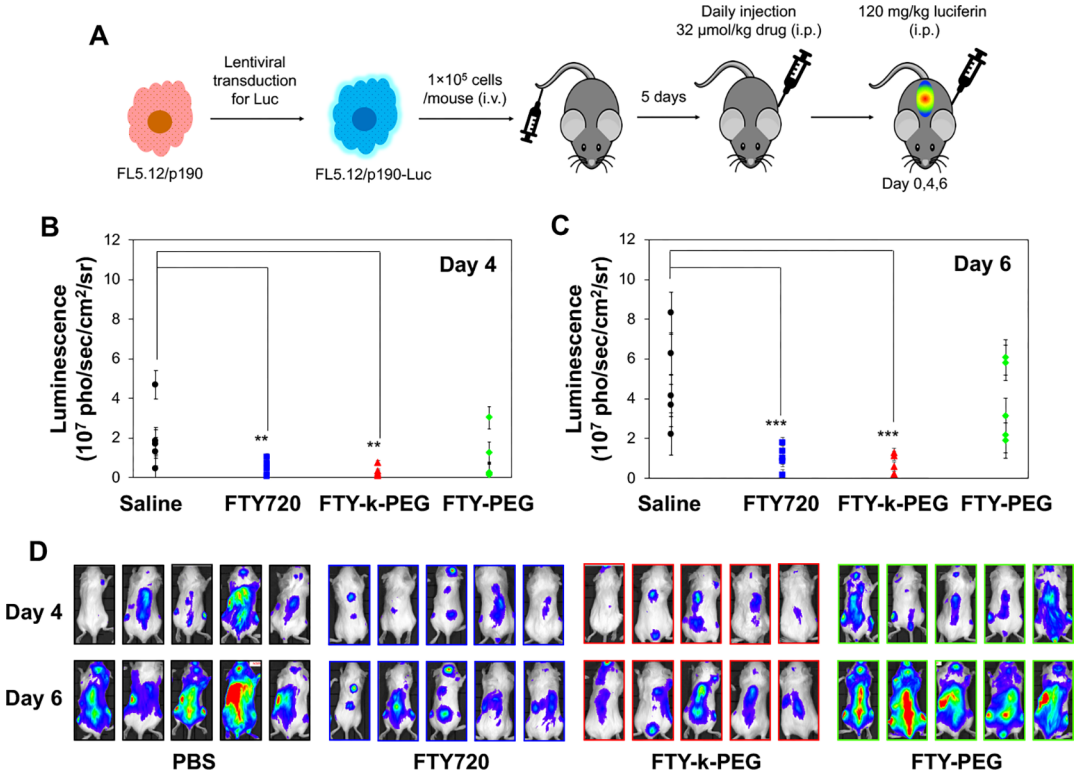

Figure 6. FTY-k-PEG maintains antileukemic effect in vivo. (A) Experimental workflow for cell transduction to express luciferase, cell administration to mice, treatment, and bioluminescent analysis. (B,C) Quantification of bioluminescence after mice were injected with FL5.12/p190 luciferase-expressing cells, and subsequently treated with either FTY720, PBS, FTY-PEG or FTY-k-PEG (32 μmol/kg) for 4 and 6 days. (D) Bioluminescent images of each group on day 4 (top row) and day 6 (bottom row) post-first treatment. $^{**}p < 0.05$, $^{***}p < 0.01$.

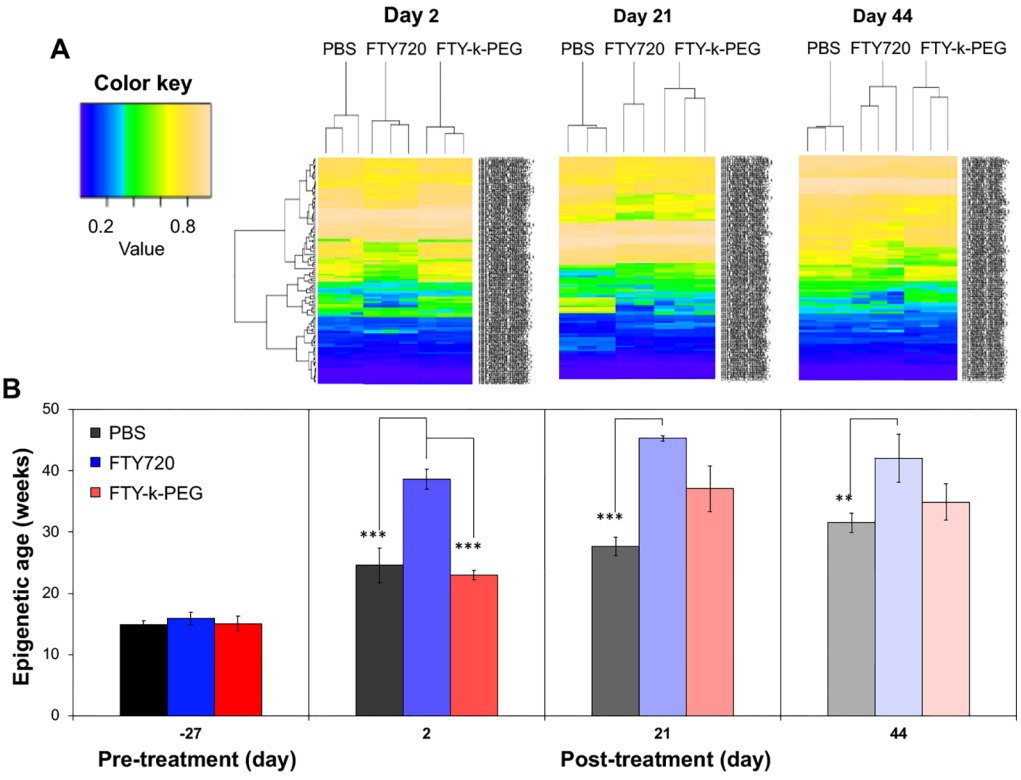

Figure 7. Healthy BALB/c mice were treated with FTY720 (10 mg/kg [32 μmol/kg]) or FTY-k-PEG (155 mg/kg [32 μmol/kg]) or PBS by daily i.p. injections for 14 days, and blood samples were taken 2 days post-first treatment, 5 days after treatment ended, and 1 month after treatment. (A) Heatmap representation of differentially methylated regions used to calculate epigenetic age at various time points. (B) Epigenetic age generated from samples analyzed using proprietary markers for DNA methylation status (n = 3).

https://dx.doi.org/10.1021/acs.bioconjchem.9b00822
Bioconjugate Chem. 2020, 31, 673−684

acid-transforming prodrug formulation is a viable option to utilize the therapeutic benefits of FTY720 against leukemia and other cancers with avoided adverse side effects. Since FTY720 is an FDA-approved drug for multiple sclerosis and is selectively toxic to cancerous cells, a viable prodrug formulation with a preserved anticancer activity with lowered toxicity is highly beneficial for fast clinical translation, not only for therapeutic efficacy but also improved quality of patient life post-treatment.[2,33,34]

Minimized Epigenetic Age by FTY-k-PEG. DNA methylation-derived biomarkers are currently gaining significant interest as changes in the epigenetic age are known to be associated with several pathological conditions including cancer[69] as well as treatment with certain chemotherapeutic drugs.[70] In attempts to explore epigenetic age as a possible means to quantitatively evaluate systemic toxicity of a drug, healthy female Balb/c mice were daily treated with i.p. injections of FTY720, FTY-k-PEG, or PBS for 2 weeks, and blood samples were drawn prior to, during, and after treatment. Epigenetic age analysis was performed using Zymo Research Corporation's DNAge Epigenetic Aging Clock service, which assesses proprietary DNA methylation patterns known to specifically correlate epigenetic age to biological age. The methylated regions used for comparative analysis with corresponding methylation value (Figure 7A) showed clear differences in epigenetic biomarkers between FTY and FTY-k-PEG, and a significant increase in epigenetic age was observed in mice treated with FTY720 but not with FTY-k-PEG, 2 days post-treatment (Figure 7B). It was previously reported that bradycardia is most prevalent in the first 2 days after FTY720 administration,[25] and it was within this time frame when the greatest difference in epigenetic age was observed with FTY-k-PEG, possibly associated with avoided bradycardia and lymphopenia (Figure 5). Although further investigation into a likely correlation between FTY720s toxicity and increased epigenetic age relative to control and FTY-k-PEG warrants further evaluation, epigenetic age analysis could be a promising way to quantitatively assess the adverse side effects of a drug at a molecular level, particularly on inflammation, disease development and progress, and other health issues.[71−73]

CONCLUSIONS

The limited clinical use of FTY720 for cancer therapy due to bradycardia and lymphopenia was addressed by an FTY720 prodrug that remains inactive during circulation but converts into its active form upon exposure to mildly acidic intracellular conditions. The prodrug engineering utilized an acid-labile cyclic ketal group to conjugated PEG, resulting in FTY-k-PEG, in an attempt to specifically inhibit phosphorylation of FTY720 that initiate the side effects. The synthetic methodology developed in this study is straightforward, scalable, and a less costly alternative to the development of an entirely new drug. FTY-k-PEG demonstrated nearly identical efficacy to free drug in BCR-Abl p190-driven leukemia model, both in vitro and in vivo, but without inducing bradycardia or lymphopenia. DNA methylation patterns known to be correlated with inflammation and disease implicated lower epigenetic damage by FTY-k-PEG. This study demonstrated that prodrug engineering to disrupt specific off-target molecular mechanisms can effectively improve the safety profile of a drug. Future studies will be done on solid tumors to exploit the acid-cleavable prodrug for targeted anticancer effects, to elucidate the interactions of the prodrug at the molecular level, and to develop a combination therapy for synergistic cancer therapy.

EXPERIMENTAL SECTION

Materials. All chemicals purchased from various vendors were used as received without further purification. FTY720·HCl was purchased from LC Laboratories (Woburn, MA). Succinimidyl PEG NHS 5K (mPEG SCM 5K) was purchased from Nanocs (Boston, MA). Anhydrous tetrahydrofuran (THF), anhydrous ethyl acetate (EtOAc), dichloromethane (DCM), anhydrous toluene, 3 Å molecular sieves, triethylamine (TEA), and pyridinium *p*-toluenesulfonate (PPTS) were purchased from Acros Organics (Morris Plains, NJ). *para*-Toluenesulfonic acid monohydrate (pTSA), anhydrous dimethylformamide (DMF), and dimethylsulfoxide (DMSO) were purchased from Sigma-Aldrich (Milwaukee, WI). Fmoc-*n*-piperidone, anhydrous magnesium sulfate, and all cell culture materials were purchased from Fisher Scientific (Hampton, NH). ^{1}H NMR spectra were obtained using a Bruker Advance 500 MHz NMR spectrometer (Billerica, MA). Electrospray mass spectra were obtained by using a Micromass LCT mass spectrometer (Milford, MA). For the determination of average molecular weight of mPEG SCM 5K and PEGylated prodrugs, an AB SCIEX MALDI TOF-TOF 5800 instrument (Framingham, MA) was used, and samples were prepared using 2,5-dihydroxybenzoic acid (Acros Organics (Morris Plains, NJ) as matrix material. The samples were irradiated with 349 nm of diode-pumped solid state Nd:YAG laser and detected on linear high mass positive mode. For the molecular weight analysis, Mn calculated using Data Explorer software (Applied Biosystems, Foster City, CA).

SYNTHESIS

FTY-TFA (2). FTY720·HCl (1.00 g, 2.9 mmol) was dissolved in 150 mL of dehydrated ethanol at room temperature. Triethylamine (1.00 mL, 7.25 mmol) was added and stirred for 25 min, followed by adding ethyl trifluoroacetate (0.450 mL, 3.7 mmol) and stirring for 24 h. Solvent was removed in vacuo, and product was separated by silica gel column chromatography (EtoAc:Hex). Yield 70.6%. ^{1}H NMR (600 MHz, DMSO-d_6, 25 °C), δ 8.05 (s, 1H), 7.08 (m, 4H), 4.85 (t, 2H), 3.69 (dd, 2H), 3.55 (m, 2H), 2.49 (m, 4H), 1.92 (m, 2H), 1.54 (m, 2H), 1.27 (m, 10H), 0.87 (t, 3H). ^{13}C NMR (600 MHz, DMSO-d_6, 25 °C), δ140.03, 139.85, 128.65, 128.46, 62.16, 60.07, 36.96, 34.69, 31.55, 31.24, 31.03, 28.80, 28.64, 28.31, 22.05, 13.91 (ESI) calcd for $C_{21}H_{32}F_3NO_3$ $[M + Na]^+$ 426.459, found 426.211

mkFTY-TFA (3). PPTS (0.053 g, 0.213 mmol) was added to FTY-TFA (**2**) (0.86 g, 2.13 mmol) in 25 mL of anhydrous THF and stirred for 10 m. Molecular sieves (5 Å) (10 g) were added, and the mixture was stirred for 10 min in an ice bath, followed by adding 2-methoxypropene (1.22 mL, 12.7 mmol) and being stirred for 2 h. The reaction was quenched with triethylamine (0.029 mL), and product was purified via extraction with DI water, dried over anhydrous MgSO4. Yield 86%. ^{1}H NMR (600 MHz, DMSO-d_6, 25 °C), δ 8.08 (s, 1H), 7.08 (m, 4H), 3.16 (q, 4H), 3.11 (s, 6H), 2.46 (m, 4H), 1.54 (m, 4H), 1.27 (m, 22H), 0.87 (t, 3H). (ESI) calcd for $C_{29}H_{48}F_3NO_5$ $[M + Na]^+$ 570.680, found 570.472

mkFTY (4). mkFTY-TFA (**3**) was dissolved in 3N NaOH in 1:1 water:methanol for 6 h, and product was extracted 9 times with dichloromethane. Yield 61%. ^{1}H NMR (600 MHz,

https://dx.doi.org/10.1021/acs.bioconjchem.9b00822
Bioconjugate Chem. 2020, 31, 673−684

DMSO-d_6, 25 °C), δ 7.08 (m, 4H), 3.16 (q, 4H), 3.11 (s, 6H), 2.46 (m, 2H), 1.54 (m, 4H), 1.27 (m, 22H), 0.87 (t, 3H)^{13}C NMR (600 MHz, DMSO-d_6, 25 °C), δ128.18, 127.98, 99.17, 64.54, 53.53, 47.82, 37.43, 37.18, 34.74, 31.25, 31.05, 28.82, 28.65, 24.31, 24.25, 22.07, 13.94 (ESI) calcd for $C_{27}H_{49}NO_4$ $[M + Na]^+$ 474.672, found 474.724.

Fmoc-kFTY-TFA (5). In toluene (10 mL), *p*-toluenesulfonic acid monohydrate (424 mg, 2.2 mmol) was heated to reflux for 1 h, while water was distilled off by condensation. FTY-TFA (**2**) (700 mg, 1.7 mmol) and 4-Fmoc-piperidone (1.4 g, 5.2 mmol) were added in 10 mL of toluene and heated to 110 °C for 6 h using a Dean−Stark trap. Solvent was removed under a reduced pressure, and product was purified by column chromatography with eluting solvent gradient of hexane to 5:3 hexane:ethyl acetate (1% TEA to prevent hydrolysis). Yield 52%. ^{1}H NMR (600 MHz, DMSO-d_6, 25 °C), δ 7.91 (d, 2H), 7.64 (d, 2H), 7.44 (t, 2H), 7.36 (t, 2H), 7.10 (d, 2H), 7.05 (d, 2H), 4.40 (m 2H), 4.25 (t, 1H), 4.18 (d, 2H), 3.83 (d, 2H), 3.22 (d, 2H), 2.41 (m, 2H), 1.85 (m, 4H), 1.55 (m, 4H), 1.27 (m, 10H), 0.87 (t, 3H). ^{13}C NMR (600 MHz, DMSO-d_6, 25 °C), δ155.02, 144.24, 141.28, 128.15, 127.63, 125.47, 120.61, 67.04, 47.36, 36.99, 35.18, 29.32, 29.11, 20.48, 14.31 (ESI) calcd for $C_{41}H_{49}F_3N_2O_5$ $[M + Na]^+$ 729.823, found 729.874

kFTY-TFA (6). Fmoc-kFTY-TFA (**5**) (0.100 g, 0.141 mmol) was dissolved in anhydrous THF (1.4 mL), and piperidine (5% v/v, 0.069 mL) was added, and the solution was stirred at room temperature for 24 h. Upon disappearance of starting materials as monitored by TLC, solvent was removed under reduced pressure. Crude product was dissolved in methylene chloride and purified by column chromatography using ethyl acetate containing 1% TEA, obtaining product as a light yellow oil. Yield 61.18%. ^{1}H NMR (600 MHz, $CDCl_3$, 25 °C), δ 7.01 (d, 2H), 6.97(d, 2H), 6.50 (s, 1H), 3.90 (d, 2H),3.67 (d, 2H), 2.87 (t, 2H), 2.77 (t, 2H), 2.48 (t, 2H), 2.43 (t, 2H), 1.99 (m, 2H), 1.89 (m, 2H), 1.66 (t, 2H), 1.50 (m, 2H), 1.21 (m, 10H), 0.80 (t, 3H). ^{13}C NMR (600 MHz, DMSO-d_6, 25 °C), δ162.26, 156.09, 139.74, 138.57, 128.25, 127.89, 116.55, 96.51, 69.7, 62.96, 54.47, 42.45, 35.9, 35.76, 34.72, 32.41, 31.25, 31.02, 30.76, 28.82, 28.63, 27.85, 22.06, 13.94 (ESI) calcd for $C_{26}H_{39}F_3N_2O_3$ $[M + H]^+$ 485.602, found 485.746.

kFTY (7). kFTY-TFA (**6**) (100 mg, 0.2 mmol) in 6N NaOH with a minimal amount of methanol used for solubility was stirred overnight at room temperature. Product was extracted with dichloromethane 9 times, and solvent was removed under a reduced pressure. Product was obtained as a white solid. Yield 77%. ^{1}H NMR (600 MHz, DMSO-d_6, 25 °C), δ 7.07 (d, 4H), 3.59 (d, 2H), 3.41 (d, 2H), 2.62 (m, 4H), 2.53 (m, 2H), 2.42 (m, 1H),1.78 (m, 4H), 1.65 (m, 4H), 1.56 (m, 2H), 1.52 (t, 2H), 1.24 (m, 10H), 0.84 (t, 3H). ^{13}C NMR (600 MHz, DMSO-d_6, 25 °C), δ128.35, 128.01, 48.10, 37.14, 34.73, 31.25, 31.04, 28.82, 28.65, 27.87, 22.07, 13.94 (ESI) calcd for $C_{24}H_{40}N_2O_2$ $[M + H]^+$ 389.594, found 389.688.

FTY-k-PEG (8). kFTY-TFA (**6**) (75 mg, 0.155 mmol) dissolved in anhydrous dichloromethane (2 mL) was mixed with trimethylamine (432 μL, 3.1 mmol), followed by stirring for 5 min. After mPEG SCM 5K (462 mg, 0.093 mmol) was added and stirred overnight, product was obtained as white solid. Yield 100%. MALDI-TOF Average M_n = 5628.7 g/mol (mPEG SCM 5K average M_n = 5171.1 g/mol). Crude TFA-FTY-k-PEG (150 mg, 0.155 mmol) obtained in the prior reaction without further purification was dissolved in 6N NaOH (2 mL) and stirred for 24 h, then diluted to 50 mL using deionized water and dialyzed overnight using a 2000 MWCO dialysis cassette (Fisher Scientific, Hampton, NH). Product was lyophilized to yield a white powder. Yield 77% . MALDI-TOF Average M_n = 5496.3 g/mol.

METHODS

FTY-k-PEG Hydrolysis and FTY720 Release. FTY-k-PEG (14 mg) was dissolved separately in 1 mL of deueterated acetate buffer (pH 5.0) and 1 mL of deuterated Tris-HCL buffer (pH 7.4) in D_2O and shaken at 37 °C for 48 h. ^{1}H NMR spectra were taken at 0, 6, 28, and 48 h, and hydrolysis rate was determined by integration of the peak at 2.23 ppm as it shifted to 1.91 ppm. Half-life was calculated using the Arrhenius equation, $t_{1/2} = \ln(k)/2$

Cell Culture. Murine IL-3-dependent proB-cell lymphoid FL5.12 cells and FL5.12/BCR-Abl p190 cells were gifted from Dr. Aimee Edinger (UC Irvine). FL5.12/p190 cells were transduced to express firefly luciferase by lentiviral vectors purchased from Capital Bioscience (Gaithersberg, MD). FL5.12/p190 and luciferase-expressing FL5.12/p190 cells (FL5.12/p190/Luc cells) were maintained at 250 000−800 000 cells/mL in RPMI 1640 media containing 10% (v/v) FBS and 1% (v/v) streptomycin−penicillin. FL5.12 cells were cultured in the same media supplemented with 5 ng/mL IL3. All cells were cultured at 37 °C with 5% CO_2 and 100% humidity.

Cell Viability. FL5.12 and FL5.12/p190 cells were seeded in a 48-well plate at a density of 4.0×10^4 cells/well with or without IL-3 (5 ng/mL) (Thermo Fisher, Waltham, MA). After incubation in varying concentrations of FTY720 and FTY-prodrugs for 24 h and rinsed with PBS, the cells were counted by flow cytometry (Guava Technologies, Hayward, CA) using Guava ViaCount Reagent (Guava Technologies, Hayward, CA) according to the manufacturer's recommended protocols.

Nutrient Transporter Expression. Surface 4F2hc expression was measured using phycoerythrin (PE)-conjugated rat antimouse 4F2hc antibody (BD Pharmingen, San Diego, CA); analysis by flow cytomery was restricted to viable cells. PE-conjugated mouse IgG1, κ (BD Pharmingen) was used as an isotype control. Cells were analyzed on a BD LSR II flow cytometer (BD Biosciences, San Jose, CA) and with FlowJo software (Treestar, Ashland, OR).

Heart Rate. Male C57BL/6 mice age 4−6 months were surgically implanted with DSI TA-ETAF20 electrocardiographic telemetry devices (Data Sciences International, St. Paul, MN) in the mouse's abdominal cavity with biopotential leads sutured in place in the chest wall. The electrocardiographic data was collected and recorded using the PhysioTel telemetry system and Dataquest A.R.T. 4.0 software (Data Sciences International). Mice were permitted a two week-long recovery after surgery before initiation of baseline telemetry recordings. Heart rate was calculated from ECG data taken in the freely moving, conscious mice. Mice (n = 3) were intraperitoneally treated with a single dose of vehicle (0.9% saline or 20% acidified DMSO in 0.9% saline), 10 mg/kg FTY720, or 155 mg/kg FTY-k-PEG, and heart rate was continuously monitored for 10 h. Mice were rested for 2 weeks at which point the experiment was repeated with the mice assigned to the alternate group. These experiments were performed as previously reported[29] in accordance with all national or local guidelines and regulations and were approved

https://dx.doi.org/10.1021/acs.bioconjchem.9b00822
Bioconjugate Chem. 2020, 31, 673−684

by the UCI Institutional Animal Care and Use Committee (IACUC).

Lymphocyte Sequestration. Female 8−24 week old C57BL6 mice were intraperitoneally injected with vehicle (0.9% saline or 20% acidified DMSO in 0.9% saline), 10 mg/kg (32 μmol/kg) FTY720, or 155 mg/kg FTY-k-PEG (32 μmol/kg). After 12 h, blood was collected from the retro-orbital sinus under ketamine/xylazine anesthesia. Whole blood (10 μL) was added to 190 μL of ACK red blood cell lysis buffer. The mixture was incubated at RT for 3−5 min at 37 °C, and the white blood cells were recovered by centrifugation. Nucleated cells (Hoechst33342-positive) were counted using a hemocytometer to obtain the white blood cell count. Separately, 50 μL of whole blood was added to 1 mL of ACK red blood cell lysis buffer and incubated for 3−5 min at RT. Cells were washed with 2% fetal calf serum (FCS, Atlanta Biologicals (Flowery Branch, GA) in PBS with 0.05% NaN3 (Sigma-Aldrich (Milwaukee, WI)), and red blood cell lysis was repeated. Tubes were decanted and resuspended in 100 μL of 10% FCS in PBS with 0.05% NaN3 and directly conjugated antibodies against B220, CD4, or CD8 (all from Biolegend, San Diego, CA) for 30 min on ice. Cells were analyzed on a BD LSR II flow cytometer; the analysis was restricted to live cells (DAPI-negative). These experiments were performed in accordance with all national or local guidelines and regulations and were approved by the UCI IACUC.

In Vivo Bioluminescence Imaging. In an immune competent syngeneic model, 6−7 weeks old Balb/c female mice were intravenously injected with FL5.12/p190/Luc cells (1.0×10^5 cells per mouse) in the tail vein. After 5 days, the mice received daily i.p. injections of FTY720, FTY-k-PEG, FTY-PEG (all at a dose of 32 μmol/kg) or PBS for 5 days (n = 5). Mice were placed under anesthesia using isoflurane (Patterson Veterinary, Greeley, CO) and interperitoneally injected with 120 mg/kg of synthetic firefly luciferin (Promega, Madison, WI) in PBS at a concentration of 20 mg/mL immediately prior to bioluminescence imaging with an IVIS Lumina system (Caliper Life Sciences, Hopkinton, MA) for 4 min. Mice were under anesthesia for the entire duration of imaging and bioluminescence signal intensities in mice were quantified using Living Image 3.2 software associated with the imaging system. These experiments were performed as reviewed and approved by the UCI IACUC.

DNAge (Epigenetic Aging Clock) Analysis. Blood samples (100 μL) were collected in triplicate from healthy female BALB/c mice treated as described above. Upon immediate preservation in DNA/RNA Shield (Zymo Research, Irvine, CA), genomic DNA was purified using Quick-DNA Plus Kit (Zymo Research) as instructed by the manufacturer. Sample library preparation and data analysis for mouse DNAge(epigenetics aging clock) were performed by service provider (Zymo Research). Briefly, genomic DNA (200 ng) was bisulfite-converted using EZ DNA Methylation-Lightning Kit (Zymo Research). Bisulfite-converted DNA libraries for targeted bisulfite sequencing platform, called SWARM (Simplified Whole-panel Amplification Reaction Method), were sequenced on a HiSeq 1500 sequencer for >1000× coverage. Sequence reads were identified using Illumina base calling software (San Diego, CA) and aligned to the reference genome using Bismark, an aligner optimized for bisulfite sequence data and methylation calling. The methylation level of each sampled cytosine was estimated as the number of reads reporting a C, divided by the total number of reads reporting a C or T. DNA methylation levels of >500 age-related CpG loci were used for age prediction using Zymo Research's proprietary human DNAge algorithms:

A penalized regression model's coefficients b_0, b_1, ... , b_n relate to transformed age as follow:

$$F(\text{chronological age}) = b_0 + b_1\text{CpG}_1 + \ldots + b_n\text{CpG}_n + \text{error}$$

DNAge is estimated as follow:

$$\text{DNAge}^{\text{TM}} = F(b_0 + b_1\text{CpG}_1 + \ldots + b_n\text{CpG}_n)^{-1}$$

Animal Studies. These experiments were performed as reviewed and approved by the UCI IACUC.

Statistical Analysis. All data collected in duplicate or triplicate and represented as mean ± standard deviation. Statistical analysis was performed with Student's t-test with statistical significance at p-values lower than 0.05.

■ ASSOCIATED CONTENT

Supporting Information

The Supporting Information is available free of charge at https://pubs.acs.org/doi/10.1021/acs.bioconjchem.9b00822.

Additional synthetic scheme, MALDI-TOF spectra, in vitro, and in vivo data (PDF)

■ AUTHOR INFORMATION

Corresponding Author

Young Jik Kwon − *Department of Pharmaceutical Sciences, Department of Chemical and Biomolecular Engineering, Department of Molecular Biology and Biochemistry, and Department of Biomedical Engineering, University of California, Irvine, California 92697, United States;* orcid.org/0000-0003-4086-6995; Phone: 949-824-8714; Email: kwonyj@uci.edu

Authors

Jessica A. Kemp − *Department of Pharmaceutical Sciences, University of California, Irvine, California 92697, United States*

Andrew Keebaugh − *Department of Medicine, University of California, Irvine, California 92697, United States*

Julius A. Edson − *Department of Chemical and Biomolecular Engineering, University of California, Irvine, California 92697, United States*

David Chow − *Department of Pharmaceutical Sciences, University of California, Irvine, California 92697, United States*

Michael T. Kleinman − *Department of Medicine, University of California, Irvine, California 92697, United States*

Yap Ching Chew − *Zymo Research Corporation, Irvine, California 92604, United States*

Alison N. McCracken − *Department of Developmental and Cell Biology, University of California, Irvine, California 92697, United States*

Aimee L. Edinger − *Department of Developmental and Cell Biology, University of California, Irvine, California 92697, United States*

Complete contact information is available at: https://pubs.acs.org/10.1021/acs.bioconjchem.9b00822

Funding

This study was financially supported by University of California Cancer Research Coordinating Committee

(CRCC) (CRR-14-201514). ALE was supported by the American Cancer Society (RSG-11-111-01-CDD).

Notes

The authors declare no competing financial interest.

■ ABBREVIATIONS

FTY, (FTY720); FTY-k-PEG, (FTY720-ketal-polyethylene glycol); kFTY, (ketal-functionalized FTY720); Luc, (luciferase); mkFTY, (methyl- ketal-functionalized FTY720); PEG, (polyethylene glycol); PP2A, (protein phosphatase 2A); SCM-PEG, (succinimidyl carboxyl methyl ester polyethylene glycol); TFA, (trifluoroacetamide)

■ REFERENCES

(1) Peer, D., Karp, J. M., Hong, S., Farokhzad, O. C., Margalit, R., and Langer, R. (2007) Nanocarriers as an emerging platform for cancer therapy. *Nat. Nanotechnol. 2*, 751−760.

(2) Vasir, J. K., and Labhasetwar, V. (2005) Targeted Drug Delivery in Cancer Therapy. *Technol. Cancer Res. Treat. 4*, 363−374.

(3) Brannon-Peppas, L., and Blanchette, J. O. (2012) Nanoparticle and targeted systems for cancer therapy. *Adv. Drug Delivery Rev. 64*, 206−212.

(4) Brown, J. M., and Wilson, W. R. (2004) Exploiting tumour hypoxia in cancer treatment. *Nat. Rev. Cancer 4*, 437−447.

(5) Vanneman, M., and Dranoff, G. (2012) Combining immunotherapy and targeted therapies in cancer treatment. *Nat. Rev. Cancer 12*, 237−251.

(6) Allen, T. M. (2002) Ligand-targeted therapeutics in anticancer therapy. *Nat. Rev. Cancer 2*, 750−763.

(7) Sawyers, C. (2004) Targeted cancer therapy. *Nature 432*, 294−297.

(8) Kemp, J. A., Shim, M. S., Heo, C. Y., and Kwon, Y. J. (2016) Combo" nanomedicine: co-delivery of multi-modal therapeutics for efficient, targeted, and safe cancer therapy. *Adv. Drug Delivery Rev. 98*, 3−18.

(9) Jin, S., DiPaola, R. S., Mathew, R., and White, E. (2007) Metabolic catastrophe as a means to cancer cell death. *J. Cell Sci. 120*, 379−383.

(10) Dang, C. V. (2012) Links between metabolism and cancer. *Genes Dev. 26*, 877−890.

(11) Shin, D. M., Ro, J. Y., Hong, W. K., and Hittelman, W. N. (1994) Dysregulation of epidermal growth factor receptor expression in premalignant lesions during head and neck tumorigenesis. *Cancer Res. 54*, 3153−3159.

(12) Rabinowitz, J. D., and White, E. (2010) Autophagy and metabolism. *Science 330*, 1344−1348.

(13) Vander Heiden, M. G. (2011) Targeting cancer metabolism: a therapeutic window opens. *Nat. Rev. Drug Discovery 10*, 671−684.

(14) Selwan, E. M., Finicle, B. T., Kim, S. M., and Edinger, A. L. (2016) Attacking the supply wagons to starve cancer cells to death. *FEBS Lett. 590*, 885−907.

(15) Neviani, P., Santhanam, R., Oaks, J. J., Eiring, A. M., Notari, M., Blaser, B. W., Liu, S., Trotta, R., Muthusamy, N., Gambacorti-Passerini, C., et al. (2007) FTY720, a new alternative for treating blast crisis chronic myelogenous leukemia and Philadelphia chromosome−positive acute lymphocytic leukemia. *J. Clin. Invest. 117*, 2408−2421.

(16) Stafman, L. L., Williams, A. P., Marayati, R., Aye, J. M., Stewart, J. E., Mroczek-Musulman, E., and Beierle, E. A. (2019) PP2A activation alone and in combination with cisplatin decreases cell growth and tumor formation in human HuH6 hepatoblastoma cells. *PLoS One 14*, e0214469.

(17) De Palma, R. M., Parnham, S. R., Li, Y., Oaks, J. J., Peterson, Y. K., Szulc, Z. M., Roth, B. M., Xing, Y., and Ogretmen, B. (2019) The NMR-based characterization of the FTY720-SET complex reveals an alternative mechanism for the attenuation of the inhibitory SET-PP2A interaction. *FASEB J. 33*, 7647−7666.

(18) Oaks, J. J., Santhanam, R., Walker, C. J., Roof, S., Harb, J. G., Ferenchak, G., Eisfeld, A.-K., Van Brocklyn, J. R., Briesewitz, R., Saddoughi, S. A., et al. (2013) Antagonistic activities of the immunomodulator and PP2A-activating drug FTY720 (Fingolimod, Gilenya) in Jak2-driven hematologic malignancies. *Blood 122*, 1923−1934.

(19) Barthelemy, C., Barry, A. O., Twyffels, L., and André, B. (2017) FTY720-induced endocytosis of yeast and human amino acid transporters is preceded by reduction of their inherent activity and TORC1 inhibition. *Sci. Rep. 7*, 13816−13816.

(20) Kim, S. M., Roy, S. G., Chen, B., Nguyen, T. M., McMonigle, R. J., McCracken, A. N., Zhang, Y., Kofuji, S., Hou, J., Selwan, E., et al. (2016) Targeting cancer metabolism by simultaneously disrupting parallel nutrient access pathways. *J. Clin. Invest. 126*, 4088−4102.

(21) Romero Rosales, K., Singh, G., Wu, K., Chen, J., Janes, M. R., Lilly, M. B., Peralta, E. R., Siskind, L. J., Bennett, M. J., Fruman, D. A., and Edinger, A. L. (2011) Sphingolipid-based drugs selectively kill cancer cells by down-regulating nutrient transporter proteins. *Biochem. J. 439*, 299−311.

(22) Kerbel, R., and Folkman, J. (2002) Clinical translation of angiogenesis inhibitors. *Nat. Rev. Cancer 2*, 727−739.

(23) Priest, J. R., Ramsay, N. K., Steinherz, P. G., Tubergen, D. G., Cairo, M. S., Sitarz, A. L., Bishop, A. J., White, L., Trigg, M. E., Levitt, C. J., et al. (1982) A syndrome of thrombosis and hemorrhage complicating L-asparaginase therapy for childhood acute lymphoblastic leukemia. *J. Pediatr. 100*, 984−989.

(24) Shishavan, M. H., Bidadkosh, A., Yazdani, S., Lambooy, S., van den Born, J., Buikema, H., Henning, R. H., and Deelman, L. E. (2016) Differential Effects of Long Term FTY720 Treatment on Endothelial versus Smooth Muscle Cell Signaling to S1P in Rat Mesenteric Arteries. *PLoS One 11*, e0162029.

(25) Camm, J., Hla, T., Bakshi, R., and Brinkmann, V. (2014) Cardiac and vascular effects of fingolimod: mechanistic basis and clinical implications. *Am. Heart J. 168*, 632−644.

(26) Cohen, J. A., and Chun, J. (2011) Mechanisms of fingolimod's efficacy and adverse effects in multiple sclerosis. *Ann. Neurol. 69*, 759−777.

(27) Sanna, M. G., Liao, J., Jo, E., Alfonso, C., Ahn, M.-Y., Peterson, M. S., Webb, B., Lefebvre, S., Chun, J., Gray, N., et al. (2004) Sphingosine 1-phosphate (S1P) receptor subtypes S1P1 and S1P3, respectively, regulate lymphocyte recirculation and heart rate. *J. Biol. Chem. 279*, 13839−13848.

(28) Koyrakh, L., Roman, M. I., Brinkmann, V., and Wickman, K. (2005) The heart rate decrease caused by acute FTY720 administration is mediated by the G protein-gated potassium channel IKACh. *Am. J. Transplant. 5*, 529−536.

(29) Chen, B., Roy, S. G., McMonigle, R. J., Keebaugh, A., McCracken, A. N., Selwan, E., Fransson, R., Fallegger, D., Huwiler, A., Kleinman, M. T., et al. (2016) Azacyclic FTY720 Analogues That Limit Nutrient Transporter Expression but Lack S1P Receptor Activity and Negative Chronotropic Effects Offer a Novel and Effective Strategy to Kill Cancer Cells in Vivo. *ACS Chem. Biol. 11*, 409−414.

(30) Baer, A., Colon-Moran, W., and Bhattarai, N. (2018) Characterization of the effects of immunomodulatory drug fingolimod (FTY720) on human T cell receptor signaling pathways. *Sci. Rep. 8*, 10910.

(31) McCracken, A. N., McMonigle, R. J., Tessier, J., Fransson, R., Perryman, M. S., Chen, B., Keebaugh, A., Selwan, E., Barr, S. A., Kim, S. M., et al. (2017) Phosphorylation of a constrained azacyclic FTY720 analog enhances anti-leukemic activity without inducing S1P receptor activation. *Leukemia 31*, 669−677.

(32) DiMasi, J. A., Hansen, R. W., and Grabowski, H. G. (2003) The price of innovation: new estimates of drug development costs. *Journal of Health Economics 22*, 151−185.

(33) Freije, I., Lamouche, S., and Tanguay, M. (2019) Review of Drugs Approved via the 505(b)(2) Pathway: Uncovering Drug Development Trends and Regulatory Requirements. *Therapeutic Innovation & Regulatory Science*, 1.

(34) Rautio, J., Meanwell, N. A., Di, L., and Hageman, M. J. (2018) The expanding role of prodrugs in contemporary drug design and development. *Nat. Rev. Drug Discovery 17*, 559−587.
(35) Kihara, A., and Igarashi, Y. (2008) Production and release of sphingosine 1-phosphate and the phosphorylated form of the immunomodulator FTY720. *Biochim. Biophys. Acta, Mol. Cell Biol. Lipids 1781*, 496−502.
(36) Venkataraman, K., Thangada, S., Michaud, J., Oo, M. L., Ai, Y., Lee, Y.-M., Wu, M., Parikh, N. S., Khan, F., Proia, R. L., et al. (2006) Extracellular export of sphingosine kinase-1a contributes to the vascular S1P gradient. *Biochem. J. 397*, 461−471.
(37) Yatomi, Y., Ruan, F., Hakomori, S.-i., and Igarashi, Y. (1995) Sphingosine-1-phosphate: a platelet-activating sphingolipid released from agonist-stimulated human platelets. *Blood 86*, 193−202.
(38) Murthy, N., Thng, Y., Schuck, S., Xu, M. C., and Fréchet, J. M. J. (2002) A Novel Strategy for Encapsulation and Release of Proteins: Hydrogels and Microgels with Acid-Labile Acetal Cross-Linkers. *J. Am. Chem. Soc. 124*, 12398−12399.
(39) Zhou, S., Sha, H., Ke, X., Liu, B.-R., Wang, X., and Du, X. (2015) Combination Drug Release of Smart Cyclodextrin-Gated Mesoporous Silica Nanovehicles. *Chem. Commun. 51*, 7203−7206.
(40) Deutsch, J., Martin, A., and Lieske, H. (2007) Investigations on heterogeneously catalysed condensations of glycerol to cyclic acetals. *J. Catal. 245*, 428−435.
(41) Yan, Y., Bornscheuer, U. T., Cao, L., and Schmid, R. D. (1999) Lipase-catalyzed solid-phase synthesis of sugar fatty acid esters: removal of byproducts by azeotropic distillation. *Enzyme Microb. Technol. 25*, 725−728.
(42) You, J.-O., Guo, P., and Auguste, D. (2013) A Drug-Delivery Vehicle Combining the Targeting and Thermal Ablation of HER2+ Breast-Cancer Cells with Triggered Drug Release. *Angew. Chem., Int. Ed. 52*, 4141−4146.
(43) Kwon, H. J., Byeon, Y., Jeon, H. N., Cho, S. H., Han, H. D., and Shin, B. C. (2015) Gold Cluster-Labeled Thermosensitive Liposomes Enhance Triggered Drug Release in the Tumor Microenvironment by a Photothermal Effect. *J. Controlled Release 216*, 132−139.
(44) Song, J., Im, K., Hwang, S., Hur, J., Nam, J., Ahn, G. O., Hwang, S., Kim, S., and Park, N. (2015) DNA hydrogel delivery vehicle for light-triggered and synergistic cancer therapy. *Nanoscale 7*, 9433−9437.
(45) Chen, W., Achazi, K., Schade, B., and Haag, R. (2015) Charge-conversional and reduction-sensitive poly(vinyl alcohol) nanogels for enhanced cell uptake and efficient intracellular doxorubicin release. *J. Controlled Release 205*, 15−24.
(46) Soyez, H., Schacht, E., and Vanderkerken, S. (1996) The crucial role of spacer groups in macromolecular prodrug design. *Adv. Drug Delivery Rev. 21*, 81−106.
(47) Thambi, T., and Lee, D. S. (2019) Stimuli-responsive polymersomes for cancer therapy. *Stimuli Responsive Polymeric Nanocarriers for Drug Delivery Applications* (Makhlouf, A. S. H., and Abu-Thabit, N. Y., Eds.), pp 413−438, Chapter 15, Vol. 2: Advanced Nanocarriers for Therapeutics, Woodhead Publishing, Cambridge.
(48) Pacardo, D. B., Ligler, F. S., and Gu, Z. (2015) Programmable nanomedicine: synergistic and sequential drug delivery systems. *Nanoscale 7*, 3381−3391.
(49) Cavallaro, G., Licciardi, M., Caliceti, P., Salmaso, S., and Giammona, G. (2004) Synthesis, physico-chemical and biological characterization of a paclitaxel macromolecular prodrug. *Eur. J. Pharm. Biopharm. 58*, 151−159.
(50) Qin, P., Han, T., Yu, A. C. H., and Xu, L. (2018) Mechanistic understanding the bioeffects of ultrasound-driven microbubbles to enhance macromolecule delivery. *J. Controlled Release 272*, 169−181.
(51) Arroyo-Crespo, J. J., Arminan, A., Charbonnier, D., Balzano-Nogueira, L., Huertas-López, F., Marti, C., Tarazona, S., Forteza, J., Conesa, A., and Vicent, M. J. (2018) Tumor microenvironment-targeted poly-L-glutamic acid-based combination conjugate for enhanced triple negative breast cancer treatment. *Biomaterials 186*, 8−21.
(52) Liu, C., Li, Y., Gao, B., Li, Y., Duan, Q., and Kakuchi, T. (2018) Comb-shaped, temperature-tunable and water-soluble porphyrin-based thermoresponsive copolymer for enhanced photodynamic therapy. *Mater. Sci. Eng., C 82*, 155−162.
(53) Zhang, X., Chytil, P., Etrych, T. s., Liu, W., Rodrigues, L., Winter, G., Filippov, S. K., and Papadakis, C. M. (2018) Binding of HSA to Macromolecular p HPMA Based Nanoparticles for Drug Delivery: An Investigation Using Fluorescence Methods. *Langmuir 34*, 7998−8006.
(54) Park, N. H., Cheng, W., Lai, F., Yang, C., Florez de Sessions, P., Periaswamy, B., Wenhan Chu, C., Bianco, S., Liu, S., Venkataraman, S., et al. (2018) Addressing drug resistance in cancer with macromolecular chemotherapeutic agents. *J. Am. Chem. Soc. 140*, 4244−4252.
(55) Chytil, P., Koziolová, E., Etrych, T., and Ulbrich, K. (2018) HPMA Copolymer−Drug Conjugates with Controlled Tumor-Specific Drug Release. *Macromol. Biosci. 18*, 1700209.
(56) Freeman, H., Srinivasan, S., Das, D., Stayton, P. S., and Convertine, A. J. (2018) Fully synthetic macromolecular prodrug chemotherapeutics with EGFR targeting and controlled camptothecin release kinetics. *Polym. Chem. 9*, 5224−5233.
(57) Deslongchamps, P., Dory, Y. L., and Li, S. (2000) The relative rate of hydrolysis of a series of acyclic and six-membered cyclic acetals, ketals, orthoesters, and orthocarbonates. *Tetrahedron 56*, 3533−3537.
(58) Kirby, A. J., and Percy, J. M. (1989) Intramolecular proton-transfer catalysis of nucleophilic catalysis of acetal hydrolysis. The hydrolysis of 8-dimethylamino-1-methoxymethoxynaphthalene. *J. Chem. Soc., Perkin Trans. 2*, 907−912.
(59) Rios, F., and Smirnov, S. N. (2011) pH valve based on hydrophobicity switching. *Chem. Mater. 23*, 3601−3605.
(60) Tannock, I. F., and Rotin, D. (1989) Acid pH in tumors and its potential for therapeutic exploitation. *Cancer Res. 49*, 4373−4384.
(61) Lee, E. S., Na, K., and Bae, Y. H. (2003) Polymeric micelle for tumor pH and folate-mediated targeting. *J. Controlled Release 91*, 103−113.
(62) Edinger, A. L., and Thompson, C. B. (2002) Akt maintains cell size and survival by increasing mTOR-dependent nutrient uptake. *Mol. Biol. Cell 13*, 2276−2288.
(63) Verhoef, J. J. F., and Anchordoquy, T. J. (2013) Questioning the Use of PEGylation for Drug Delivery. *Drug Delivery Transl. Res. 3*, 499−503.
(64) Smith, R. M., and Hansen, D. E. (1998) The pH-Rate Profile for the Hydrolysis of a Peptide Bond. *J. Am. Chem. Soc. 120*, 8910−8913.
(65) Zhang, Y., and Ertl, H. C. (2016) Starved and asphyxiated: how can CD8+ T cells within a tumor microenvironment prevent tumor progression. *Front. Immunol. 7*, 1−7.
(66) Tomita, R., Todoroki, K., Maruoka, H., Yoshida, H., Fujioka, T., Nakashima, M., Yamaguchi, M., and Nohta, H. (2016) Amino acid metabolomics using LC-MS/MS: Assessment of cancer-cell resistance in a simulated tumor microenvironment. *Anal. Sci. 32*, 893−900.
(67) Budman, D. R., Berry, D. A., Cirrincione, C. T., Henderson, I. C., Wood, W. C., Weiss, R. B., Ferree, C. R., Muss, H. B., Green, M. R., Norton, L., et al. (1998) Dose and dose intensity as determinants of outcome in the adjuvant treatment of breast cancer. *J. Natl. Cancer Inst. 90*, 1205−1211.
(68) Widakowich, C., de Castro, G., De Azambuja, E., Dinh, P., and Awada, A. (2007) Side effects of approved molecular targeted therapies in solid cancers. *Oncologist 12*, 1443−1455.
(69) Durso, D. F., Bacalini, M. G., Sala, C., Pirazzini, C., Marasco, E., Bonafé, M., do Valle, Í. F., Gentilini, D., Castellani, G., Faria, A. M. C., et al. (2017) Acceleration of leukocytes' epigenetic age as an early tumor and sex-specific marker of breast and colorectal cancer. *Oncotarget 8*, 23237−23245.
(70) Baker, E. K., Johnstone, R. W., Zalcberg, J. R., and El-Osta, A. (2005) Epigenetic changes to the MDR1 locus in response to chemotherapeutic drugs. *Oncogene 24*, 8061−8075.

https://dx.doi.org/10.1021/acs.bioconjchem.9b00822
Bioconjugate Chem. 2020, 31, 673−684

(71) Feinberg, A. P. (2018) The key role of epigenetics in human disease prevention and mitigation. *N. Engl. J. Med. 378*, 1323−1334.
(72) Sakai, K., Ideta-Otsuka, M., Saito, H., Hiradate, Y., Hara, K., Igarashi, K., and Tanemura, K. (2018) Effects of doxorubicin on sperm DNA methylation in mouse models of testicular toxicity. *Biochem. Biophys. Res. Commun. 498*, 674−679.
(73) Tretyakova, N., and Wang, Y. (2019) Epigenetics in Toxicology. *Chem. Res. Toxicol. 32*, 793−793.

https://dx.doi.org/10.1021/acs.bioconjchem.9b00822
Bioconjugate Chem. 2020, 31, 673−684